Fore-aft asymmetry of the ^{2}H(n,γ)^{3}H at very low energies

H. Khalili H. Sadeghi[1)]

Department of Physics, Faculty of Science, Arak University, Arak 8349-8-38156, Iran

Abstract: We have used the recent effective field theory (EFT) which is constructed from two- and three-nucleon interactions, using minimal substitution in the momentum dependence of these interactions. We present the calculations of the fore-aft asymmetry of γ-rays in the reaction ^{2}H(n,γ)^{3}H which are based on EFT up to next-to-next-to leading order (N^{2}LO). The results are compared with the recently reported calculations and measurements of the fore-aft asymmetry of γ-rays from neutron-deuteron radiative capture. The calculated fore-aft asymmetry of the nd radiative capture process above deuteron breakup threshold is in good agreement with the available experimental data up to 20 MeV.

Key words: effective field theory, neutron-deuteron radiative capture, photonuclear observables, fore-aft asymmetry

PACS: 21.45.1v, 24.70.1s, 25.40.Lw **DOI:** 10.1088/1674-1137/37/9/094101

1 Introduction

Very low-energy radiative capture reactions involving few-nucleon systems have considerable astrophysical relevance for the studies of stellar structure evolution and big-bang nucleosynthesis. Over the last decades, photonuclear processes such as the radiative capture of ^{3}H and ^{3}He and the corresponding inverse reactions have been investigated experimentally and theoretically with considerable interest. There have been a lot of experiments using different techniques for the neutron-deuteron radiative capture [1–7] or its inverse reaction.

Capture of thermal S-wave neutrons by deuteron proceeds primarily by M_1 transitions. Because of the orthogonality of the radial component of the scattering state in the neutron-deuteron system with the dominant S component of the triton ground state, neutron capture takes place through the small S' component of the ^{3}H ground state which results in the small capture cross section value. In contrast, the radial parts of the scattering neutron-deuteron ground state are essentially identical which results in a large capture cross section [8, 9].

A variety of electromagnetic observables involving the two- and three-body nuclei are taken as a case study for the neutron-deuteron and proton-deuteron radiative captures, and the magnetic form factors of ^{3}H and ^{3}He (for a review, see Ref. [8]). The first theoretical calculations were restricted to phenomenological interactions with various approximations in the bound state wave function and the scattering states. Early consistent theoretical calculation for both the initial and the final state was done by Gibson et al. [10]. The very low-energy neutron-deuteron radiative capture process is dominated by the magnetic dipole (M_1) transition, and has been studied by several authors [11–13] in configuration-space with inclusion of three-body forces, final state interaction (FSI), conserved two- and three-body electromagnetic currents, and explicit meson exchange currents (MEC). Most recently, Marcucci et al. [13] applied two different approaches for constructing conserved two- and three-body electromagnetic currents: one is based on meson-exchange mechanisms, while the other uses minimal substitution in the explicit isospin exchange operator–momentum dependence of the two- and three-nucleon interactions. They calculated a variety of observables for the A=3 nuclear systems, cross sections as well as polarization observables in the energy range 0–20 MeV, to test their model of nuclear current operator.

The recently developed pionless effective field theory (EFT) is particularly suited for high order precision calculation [14–28]. The so-called pionless EFT in nuclear physics aspires to a systematic classification of all forces. At its heart lies the tenet that physics at those very low energies can be described by point-like interactions between nucleons only. In this approach, all particles but the nucleons themselves are considered high energy degrees of freedom and are consequently "integrated out". The resulting EFT is considerably simpler than potential models or the "pionful" version of nuclear EFT (in which pions are kept as explicit degrees of freedom), but its range of validity is reduced to typical momenta below

Received 9 October 2012

1) E-mail: H-Sadeghi@Araku.ac.ir

the pion mass. There are many processes situated at thermal energies which are both interesting in their own right and important for astrophysical applications. Recently we have calculated the cross section of radiative capture process nd$\rightarrow{}^3$Hγ by using pionless EFT [24, 25]. No new three-nucleon forces are needed up to N^{2}LO in order to achieve cut-off independent results, in addition to those fixed by the triton binding energy and nd scattering length in the triton channel. The cross section is determined to be $\sigma_{\rm tot}=(0.503\pm0.003)$mb. For neutron radiative capture and their inverse, photo-neutron reactions, experiments have the inherent selectivity of the photon, which almost exclusively excites the ΔT=1, ΔS=0 resonances, but have the disadvantage that the E_2 strength cannot be directly observed, due to the large E_1 cross section. Therefore identification of E_2 strength is performed by observing the interference between the E_1 and E_2 amplitudes. This is usually done by measuring the fore-aft asymmetries in the angular distribution of the reaction products [29].

The aim of the present paper is to extend the investigations of Refs. [24–28] to calculate the fore-aft asymmetry of ^{2}H(n,γ)^{3}H at very low energies. The emphasis is on constructing three-body currents with model-independent theory corresponding to three-nucleon interactions and comparison of our model's result with those of other model-dependent theory.

This paper is organized as follows: In Section 2, we present the theoretical framework of our calculations. The results are discussed is Section 3. Finally, our conclusions are summarized in Section 4.

2 A brief review of the theoretical framework

The proper Lagrangian including of the three-nucleon force is given by [22]

$$\mathcal{L} = N^\dagger\left(\mathrm{i}D_0+\frac{D^2}{2M_{\rm N}}\right)N-d^{\mathrm{i}\dagger}\left[\sigma_{\rm d}+\left(\mathrm{i}D_0+\frac{D^2}{4M_{\rm N}}\right)\right]d^{\mathrm{i}}-t^{\mathrm{A}\dagger}\left[\sigma_{\rm t}+\left(\mathrm{i}D_0+\frac{D^2}{4M_{\rm N}}\right)\right]t^{\rm A}+y_{\rm d}\left[d^{\mathrm{i}\dagger}\left(N^{\rm T}P(^3S_1)N\right)+h.c.\right]$$
$$+y_{\rm t}\left[t^{\mathrm{A}\dagger}\left(N^{\rm T}P(^1S_0)N\right)+h.c.\right]+\mathcal{L}_{\text{Three-Nucleonforce}}+\mathcal{L}_{\rm B}, \tag{1}$$

where $M_{\rm N}$, N, $d^{\rm i}$ and $t^{\rm A}$ are the nucleon mass, the nucleon field, two dibaryon fields corresponding to the deuteron and the spin-singlet virtual bound state in S-wave nucleon–nucleon scattering, respectively. $P(^3S_1)=\frac{1}{\sqrt{8}}\sigma^2\sigma^{\rm i}\tau^2$ and $P(^1S_0)=\frac{1}{\sqrt{8}}\sigma^2\tau^2\tau^{\rm A}$ are the projection operators, where $\boldsymbol{\sigma}$ ($\boldsymbol{\tau}$) operating in spin (isospin) space, project out the $^3S_1$ and $^1S_0$ NN partial waves, respectively. After minimal substitution, $D_\mu=\partial_\mu+\mathrm{i}eA_\mu\cdot\hat{Q}$($\hat{Q}$ is the charge operator) and gauge fixing terms for the photons, the $\mathcal{L}_{\rm B}$ is given by

$$\mathcal{L}_{\rm B} = \frac{\rm e}{2M_{\rm N}}N^\dagger(k_0+k_1\tau^3)\sigma.B$$
$$+e\frac{L_1}{M_{\rm N}\sqrt{r^{(^1S_0)}r^{(^3S_1)}}}{\rm d}_t{}^{j\dagger}d_{s3}B_j+h.c. \tag{2}$$

where $k_0=1/2(k_{\rm p}+k_{\rm n})=0.4399$ and $k_1=1/2(k_{\rm p}+k_{\rm n})=2.35294$ are the iso-scalar and iso-vector nucleon magnetic moment in nuclear magnetons, respectively. The unknown coefficient L_1, will be fixed at its leading non-vanishing order by the thermal cross section [16]. In the triton channel of the three-nucleon system, the three-body interactions are shown with strength $H(\Lambda)$ and is also required for renormalization at leading order [17]. It can be expanded as

$$\mathcal{H}(E;\Lambda) = \frac{2\mathcal{H}_0(\Lambda)}{\Lambda^2}+\frac{2\mathcal{H}_2(\Lambda)}{\Lambda^4}\ (ME+\gamma_{\rm t}^2)+\cdots, \tag{3}$$

where Λ is a momentum cutoff applied in the three-body equations discussed below and $H(\Lambda)$ a known log-periodic function of the cutoff that depends on a three-body parameter Λ_*. The deuteron wave function renormalization constant is given as the residue at the bound state pole:

$$Z_0^{-1}=\mathrm{i}\frac{\partial}{\partial p_0}\frac{1}{\mathrm{i}\Delta_{\rm d}(p)}\bigg|_{p_0=-\frac{\gamma_{\rm d}^2}{M_{\rm N}},p=0}. \tag{4}$$

By gauging the above Lagrangian and direct calculation including the leading relativistic corrections we get

$$\mathcal{L} = d_j^\dagger\left[\mathrm{i}(\partial_0+\mathrm{i}eA_0)+(\nabla-\mathrm{i}e\boldsymbol{A})^2\left(\frac{1}{4M_{\rm N}}+\frac{\gamma^2}{8M_{\rm N}^3}\right)\right.$$
$$\left.-(\partial_0+\mathrm{i}eA_0)^2\left(\frac{1}{4M_{\rm N}}\right)\right]d_j+\cdots. \tag{5}$$

One recovers the correct matrix elements of $J^\mu_{\rm em}$, in each order, to reproduce the couplings induced by Eq. (1).

The electric and magnetic transitions are shown by $E_l(^{2S+1}L_J)$ and $M_l(^{2S+1}L_J)$, where l is the total angular momentum of the photon, $l\geqslant1$, and J, L and S are the total angular momentum, the orbital angular momentum and the spin of the two-nucleons, respectively. A state with orbital angular momentum L can be described by a tensor, with components $\mathcal{R}_{i_1,i_2,\cdots,i_L}$ symmetric and traceless in each pair of indices [30]

$$\begin{aligned}
&L{=}0,\ \mathcal{R}{=}1,\\
&L{=}1,\ \mathcal{R}_i{=}\hat{p}_i,\\
&L{=}2,\ \mathcal{R}_{ij}{=}\frac{1}{2}(3\hat{p}_i\hat{p}_j{-}\delta_{ij}),\\
&L{=}3,\ \mathcal{R}_{ijk}{=}\frac{1}{2}(5\hat{p}_i\hat{p}_j\hat{p}_k{-}\hat{p}_i\delta_{jk}{-}\hat{p}_j\delta_{ik}{-}\hat{p}_k\delta_{ij}),\cdots,
\end{aligned}\tag{6}$$

where $\boldsymbol{p}=1/2(\boldsymbol{p}_1-\boldsymbol{p}_2)$ is the relative of two-nucleon momentum. The amplitude components are contracted with the dibaryon polarization vector $\boldsymbol{\eta}$ and electric or magnetic multipole transition, with the photon ith direction and the photon polarization $\boldsymbol{\epsilon}$ [30]:

$$\begin{aligned}
&E_1\ \ \epsilon_i{=}E_i,\\
&M_1\ \ (\hat{k}{\times}\hat{\epsilon})_i{=}M_i,\\
&E_2\ \ \epsilon_i\hat{k}_j{+}\epsilon_j\hat{k}_i{=}E_{ij},\cdots.
\end{aligned}\tag{7}$$

To this approximation, we show the electric dipole amplitudes $E_1(^1S_0)$, $E_1(^1D_2)$, the magnetic dipole $M_1(^3P_0)$, $M_1(^3P_1)$, $M_1(^3P_2)$, the electric quadrupole $E_2(^3P_1)$ and $E_2(^3P_2)$, and ignore the other higher multipole amplitudes. In terms of the multipole components, the electric and magnetic dipole and electric quadrupole transition amplitudes are given by [25]

$$\begin{aligned}
\chi_{E_1} &= \chi^\dagger\{E_1(^1S_0)\boldsymbol{\epsilon}{\cdot}\boldsymbol{\eta}{+}E_1(^1D_2)\epsilon_i\eta_j\mathcal{R}_{ij}\}\chi^{\rm c},\\
\chi_{M_1} &= \chi^\dagger\{M_1(^3P_0)\mathrm{i}(\boldsymbol{\sigma}{\cdot}\hat{p})\boldsymbol{\eta}{\cdot}(\hat{k}{\times}\hat{\epsilon}){+}M_1(^3P_1)\mathrm{i}(\boldsymbol{\sigma}{\times}\hat{p})\\
&\quad\cdot[\boldsymbol{\eta}{\times}(\hat{k}{\times}\hat{\epsilon}]{+}M_1(^3P_2)\mathrm{i}\epsilon_{ijk}U_{km}\eta_m\hat{k}_i\epsilon_j\}\chi^{\rm c},\\
\chi_{E_2} &= \chi^\dagger\{E_2(^3P_1)\mathrm{i}\epsilon_{ijk}\sigma_j\hat{p}_kE_{im}\eta_m\\
&\quad{+}E_2(^3P_2)\mathrm{i}\epsilon_{ijk}U_{jm}E_{km}\eta_i\}\chi^{\rm c},
\end{aligned}\tag{8}$$

with $x^{\rm c}{=}\mathrm{i}\sigma_2x^*$ and $U_{ij}{=}3/2(\sigma_i\hat{p}_j{+}\sigma_j\hat{p}_i){-}(\boldsymbol{\sigma}{\cdot}\hat{p})\delta_{ij}$.

At thermal energies the nd radiative capture proceeds through S-wave capture predominantly via magnetic dipole transition, $M_\alpha(^{2S+1}L_J)$, where $L{=}0$, $S{=}1/2,3/2$ and $\alpha{=}1$. The contribution of electric transition $E_\alpha(^{2S+1}L_J)$ for energies of less than 60 keV to the total cross section is very small. Therefore electric transition from the initial state will not be considered in low energies.

The M_1 amplitude receives contributions from the magnetic moments of the nucleon and dibaryon operators coupling to the magnetic field, which are described by the Lagrange density involving fields [15, 24]:

$$\begin{aligned}
\mathcal{L}_{\rm B} &= \frac{e}{2M_{\rm N}}N^\dagger(k_0{+}k_1\tau^3)\sigma.BN\\
&\quad{+}e\frac{L_1}{M_{\rm N}\sqrt{r^{(^1S_0)}r^{(^3S_1)}}}{d_{\rm t}^{j}}^\dagger d_{{\rm s}3}B_j{+}h.c,
\end{aligned}\tag{9}$$

where $d_{\rm t}$ is the $^3S_1$ dibaryon and $d_{\rm s}$ is the $^1S_0$ dibaryon. $k_0=1/2(k_{\rm p}+k_{\rm n})$=0.4399 and $k_1=1/2(k_{\rm p}+k_{\rm n})$=2.35294 are also the isoscalar and isovector nucleon magnetic moment in nuclear magnetons, respectively. The unknown coefficient L_1, will be fixed at its leading non-vanishing order by the thermal cross section [16]. The effective range theory (ERT) result differs from the EFT result due to the absence of a four-nucleon-one-photon operator [16] and cannot be obtained alone from nucleon-nucleon scattering data.

The radiative capture cross section nd$\rightarrow^3$Hγ at very low energy is given by [24]

$$\sigma{=}\frac{2}{9}\frac{\alpha}{v_{\rm rel}}\frac{p^3}{4M_{\rm N}^2}\sum_{iLSJ}[|\widetilde{\chi}_i^{LSJ}|^2],\tag{10}$$

where

$$\widetilde{\chi}_i^{LSJ}{=}\frac{\sqrt{6\pi}}{p\mu_{\rm N}}\sqrt{4\pi}\chi_i^{LSJ},\tag{11}$$

with χ standing for either E or M and $\mu_{\rm N}$ being in nuclear magneton and p being the momentum of the incident neutron in the center of mass.

The derivation of the integral equation describing neutron-deuteron scattering has been discussed before [18, 24]. We present here only the results. Nuclear interaction processes are calculated perturbatively with the small expansion parameter Q which is the ratio of the light to heavy scales. The light scales include the inverse S-wave nucleon-nucleon scattering length in the $^1S_0$ channel, the deuteron binding momentum in the $^3S_1$ channel, the magnitude of the nucleon external momentum p in the two-nucleon center-of-mass frame, and the momentum transfer to the two-nucleon system. The heavy scale is set by the pion mass m_π.

Neutron-deuteron scattering amplitude including the new term generated by the two-derivative three-body force is shown schematically in Fig. 1. This channel is expected to be more sensitive to the short range physics in general, and in fact the three-body interaction is needed at leading order to ensure correct renormalization. For calculations, the amplitude $t_{i(j)}$ describe the $d_{\rm t}{+}N{\rightarrow}d_{\rm s}{+}N(d_{\rm t}{+}N{\rightarrow}d_{\rm t}{+}N)$ process and is written as an integral equation form [17]

$$\begin{aligned}
t_{i(j)}(p,k) &= \frac{1}{4}[3\mathcal{K}(p,k){+}2\mathcal{H}(E,\Lambda)]\\
&\quad{+}\frac{1}{2\pi}\int_0^\Lambda \mathrm{d}qq^2[\mathcal{D}_{i(j)}(q)[\mathcal{K}(p,q)\\
&\quad{+}2\mathcal{H}(E,\Lambda)]t_{i(j)}(q){+}\mathcal{D}_{j(i)}(q)[3\mathcal{K}(p,q)\\
&\quad{+}2\mathcal{H}(E,\Lambda)]t_{j(i)}(q)],
\end{aligned}\tag{12}$$

where

$$\mathcal{D}_{i(j)}(q){=}\mathcal{D}_{i(j)}\left(E{-}\frac{q^2}{2M},q\right)$$

are the propagators of deuteron. k denotes the initial (on-shell) relative momentum of the deuteron and the third nucleon, and p the final (off-shell) momentum. There is no real bound state in the spin singlet channel of the two-nucleon system. For the spin-triplet or spin-singlet S-wave channel, one replaces the two-boson binding momentum γ and effective range ρ by the deuteron binding momentum $\gamma_t = 45.7025$ MeV or the scattering length $a_s = 1/\gamma_s = -23.714$ fm and the effective range ρ_t=1.764fm or r_s=2.73 fm, at zero momentum [17].

We now turn to the Faddeev integral equation to be used in the M_1 calculation. The Faddeev equation has been solved for the triton bound state to some order (e.g. LO), then the Faddeev amplitudes are taken and sandwich the photon-interactions with nucleons between them when the photon kernel is expanded to the same order. The same procedure will also be done separately for calculation at NLO and N^{2}LO orders. Finally the wave function renormalization in each order will be done (for more details, see Ref. [24, 25]).

The diagrams in Fig. 2 represent the contribution of electromagnetic interaction with nucleon, deuteron, four-nucleon-magnetic-photon operator described by a coupling between the $^3S_1$-dibaryon and $^1S_0$-dibaryon and a magnetic photon. As mentioned in the introduction, in another paper [24], we have presented a detailed schematic of these diagrams in neutron-deuteron radiative capture for ($20 \leqslant E \leqslant 200$ keV) up to N^{2}LO. Photon direct interaction with exchanged nucleon is shown in Fig. 2(c). For this interaction, we have $p.A$ and in very low energy relevant to BBN, this particular contribution has been ignored.

The last diagrams in Fig. 2 with insertion of photon to H_2 vertices is drawn for one possibility when E_2 in higher energies is considered. The parameter H_2 is the strength of the three-nucleon interaction with two derivatives (for more details see [24, 25]).

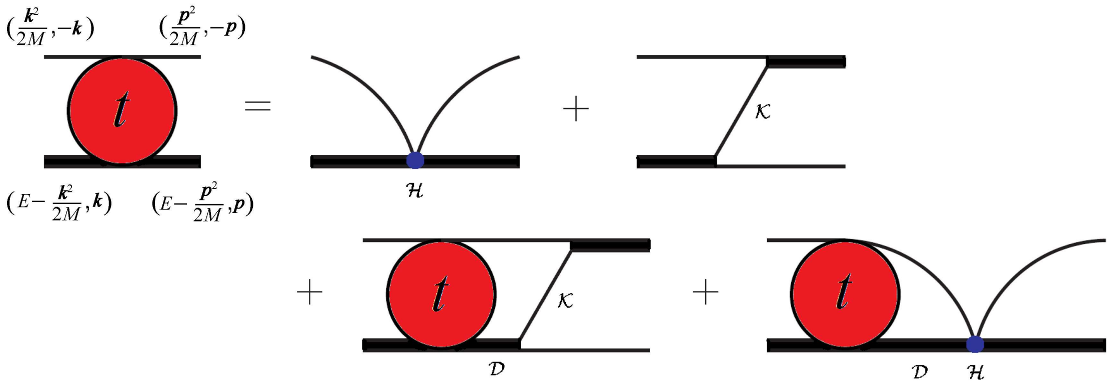

Fig. 1. The coupled Faddeev equation for nd-scattering. The thick solid line: propagator of the two intermediate auxiliary fields D_s and D_t, denoted by $\mathcal{D}$; $\mathcal{K}$: the propagator of the exchanged nucleon; $\mathcal{H}$: the three-body force.

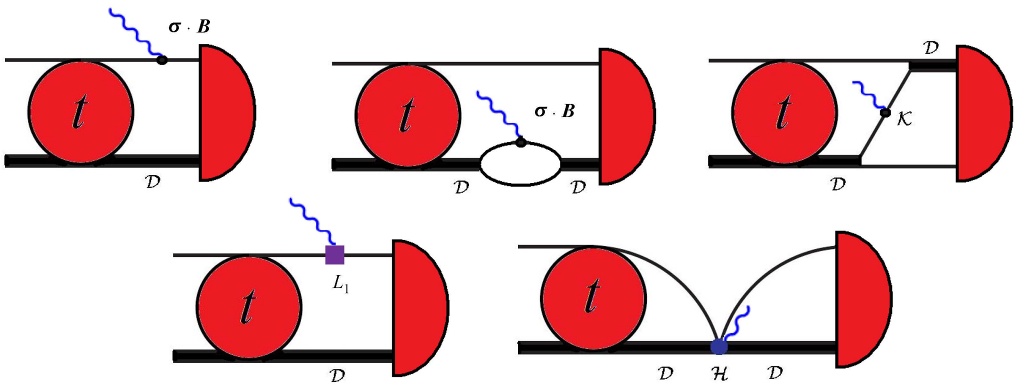

Fig. 2. The Faddeev equation for nd-radiative capture up to N^{2}LO. The circles indicate the insertion of nd-scattering amplitude up to LO from Fig. 1 (only up to the first line of perturbative expansion of the Faddeev equation (Fig. 1)). The three-body interactions are shown with strength $H(\Lambda)$. The wavy line shows photon and small circles show the magnetic photon interaction. The photon is minimally coupled. The semi-circles show the final triton bound state. The remaining notation is shown as in Fig. 1.

For triton channel, the on-shell amplitude $t_{\rm t}(k,k)$ is given by

$$T(k)=Zt_{\rm t}(k,k). \tag{13}$$

where $Z=\dfrac{8\pi\gamma}{M}(1+\gamma\rho+(\gamma\rho)^2+\cdots)$ is the wave function renormalization. To complete the NLO calculation the wave function renormalization constant Z is found from

$$\begin{aligned}\frac{1}{Z} &= \frac{1}{Z_0+Z_1}\simeq\frac{1}{Z_0}-\frac{Z_1}{Z_0^2}\\ &= \frac{1}{Z_0}-{\rm i}\frac{\partial}{\partial p_0}{\rm i}\mathcal{I}_{\rm d}(p_0,\boldsymbol{p})\Big|_{p_0=E=-E_B}\end{aligned} \tag{14}$$

and thus $Z_1=Z_0^2$.

We solve the integral equation by the insertion of Q in the integral equation and iteration of the kernel. The H_0 is determined from the $^2S_{\frac{1}{2}}$ scattering length $a_3=(0.65\pm0.04)$ fm [19]. For calculations up to LO and NLO orders, the $\rm H_0$ is the only three-body force entering. At N^{2}LO, the $\rm H_2$ is required. At this order of calculations, it is determined by the triton binding energy B_3=8.48 MeV.

The so-called fore-aft asymmetry, in the angular distribution of the cross section, is defined by

$$a_{\rm s}=\frac{\sigma(54.7^\circ)-\sigma(125.3^\circ)}{\sigma(54.7^\circ)+\sigma(125.3^\circ)}, \tag{15}$$

where $\theta_{\rm c.m.}=54.7^\circ(125.3^\circ)$ are the γ-N scattering angles.

3 Results and discussion

The Faddeev integral equation is numerically solved up to N^{2}LO. The values $\hbar c$=197.327 MeV fm, and mass of M = 938.918 MeV for nucleon are used. For the nucleon-nucleon triplet channel, a deuteron binding energy (momentum) of B=2.225 MeV ($\gamma_{\rm d}$=45.7066 MeV) is used. For the NN singlet channel, a residue of $Z_{\rm d}$ = 1.690 (3) is used. The $^1S_0$ scattering length is chosen to be $a_{\rm s}=-23.714$ fm. L_1 is found to be -4.5 fm, after fixing the leading non-vanishing order in the thermal cross section of neutron-proton radiative capture [16].

The ^{2}H(n,γ)^{3}H fore-aft asymmetry resulting from our calculation up to N^{2}LO and from that of Ref. [13, 31] is compared with the existing experimental data in Fig. 3.

In this figure, we have compared two different approaches for constructing conserved two- and three-body electromagnetic currents: one is based on modern nucleon-nucleon potentials, while the other uses minimal substitution and gauge invariant EFT of the three-nucleon systems. In the AV18/UIX potential model, one has constructed a realistic model for the three-body electromagnetic current satisfying the current conservation relation with the Urbana or Tucson-Melbourne three-nucleon interactions.

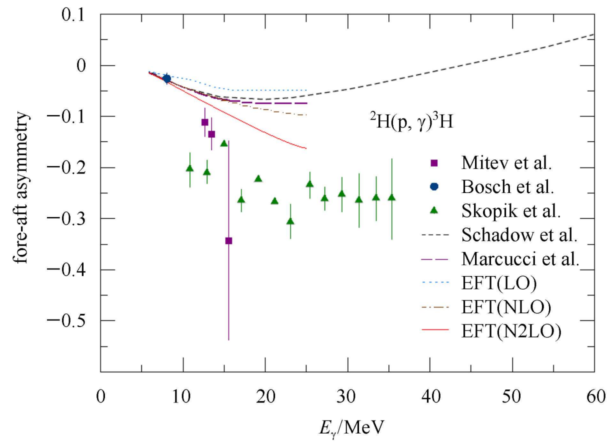

Fig. 3. Fore-aft asymmetry for nd radiative capture as function of the energy, obtained with the EFT up to N^{2}LO in comparison with the AV18/UIX (gauge invariant) Hamiltonian model current. The results of the calculation have also been reported (the dashed lines [31] and the long dashed lines [13]). The experimental data are from Refs. [1, 6, 32].

For neutron-deuteron radiative capture, the description of the angular distribution is not as good. For energies above ~20 MeV all theoretical results give a much smaller asymmetry in comparison with the experimental data. For this energy range, the calculated result shows a large discrepancy from the experimental data. These differences could be due to the problems in the analysis of the data to extract the experimental values of fore-aft asymmetry. There are also inconsistencies between the asymmetries given in Refs. [5, 6], therefore it is likely that these discrepancies are due to the experimental problems.

For higher energies, the M_1 contribution is not likely to solve the problem, since it is only expected to have an effect at extreme angles or at very low energies. It should be noted that three-nucleon forces are not expected to solve the problem since the angular distribution shows no potential dependence. A possible solution could be the inclusion of higher multipoles in the calculation at higher energies.

By estimation of the sensitivity to short-distance physics, one can provide a reasonable error analysis, by employing a momentum cut-off Λ in the solution of the Faddeev equation and varying it between the breakdown-scale $\Lambda_{\not\pi}$ to ∞. All physical observables must be independent of cut-off (Λ), up to the order of the expansion.

4 Summary and conclusion

In this paper we have calculated the fore-aft asymmetry of ^{2}H(n,γ)^{3}H process up to N^{2}LO below E=25 MeV. By comparing with our calculations using EFT, we have shown that our theoretical curve up to N^2LO in comparison with other theoretical methods, is in good agreement with the available experimental data. It is also shown that the angular distribution is insensitive to the employed interaction, we do not expect large effects of three-nucleon forces.

In conclusion, satisfactory agreement between theories and some experiments for the nd radiative capture observables of above the deuteron breakup threshold up to 20 MeV has been found. Some discrepancies, however, persist in the vector polarization observables at forward angles. The results converge order by order in low energy perturbative expansion and cut-off independently at each order. We notice that our calculation has a systematic error which is now smaller than the experimental error bar.

References

1 Bösch R B, LANG J, Mülle R, Wölfli W. Phys. Lett., 1964, **8**: 120
2 Kosiek R, Müller D, Pfeiffer R. Phys. Lett., 1966, **21**: 199
3 Pfeiffer R, Zeitschr F. Phys., 1968, **208**: 129
4 Faul D D, Berman B L, Meyer P, Olson D L. Phys. Rev. Lett., 1980, **44**: 129
5 Skopik D M et al. Phys. Rev. C, 1981, **24**: 1791
6 Mitev G, Colby P, Roberson N R, Weller H R. Phys. Rev. C, 1986, **34**: 389
7 Mösner J, Möller K, Pilz W, Schmidt G, Stiehler T. Few-Body Syst., 1986, **1**: 83
8 Carlson J, Schiavilla R. Rev. Mod. Phys., 1998, **70**: 743
9 Pastore S, Schiavilla R, Goity J L. Phys. Rev. C, 2008, **78**: 064002
10 Gibson B F, Lehman D R. Phys. Rev. C, 1975, **11**: 29
11 Friar J L, Gibson B F, Payne G L. Phys. Lett. B, 1990 **251**: 11
12 Viviani M, Schiavilla R, Kievsky A. Phys. Rev. C, 1995, **54**:534
13 Marcucci L E et al. Phys. Rev. C, 2005, **72**: 014001
14 Kaplan D B, Savage M J, Wise M B. Nucl. Phys. B, 1998, **534**: 329
15 Beane S R, Savage M J. Nucl. Phys. A, 2001, **694**: 511
16 CHEN J W, Rupak G, Savage M J. Phys. Lett. B, 1999, **464**: 1
17 Bedaque P F, Hammer H W, Van Kolck U. Phys. Rev. Lett., 1999, **82**: 463; Nucl. Phys. A, 1999, **646**: 444
18 Bedaque P F, Hammer H W, Van Kolck U. Nucl. Phys. A, 2000, **676**: 357
19 Hammer H W, Mehen T. Phys. Lett. B, 2001, **516**: 353
20 Bedaque P F, Grießhammer H W. Nucl. Phys. A, 2000, **671**: 357
21 Gabbiani F, Bedaque P F, Grießhammer H W. Nucl. Phys. A, 2000, **675**: 601
22 Konig S, Hammer H W. Phys. Rev. C, 2011, **83**: 064001
23 Ando S, Birse M C. J. Phys. G: Nucl. Part. Phys., 2010, **37**: 105108
24 Sadeghi H, Bayegan S. Nucl. Phys. A, 2005, **753**: 291
25 Sadeghi H, Bayegan S, Grießhammer H W. Phys. Lett. B, 2006, **643**: 263
26 Sadeghi H. Phys. Rev. C, 2007, **75**: 044002
27 Sadeghi H, Bayegan S. Few-Body Systems, 2010, **47**: 167
28 Sadeghi H, Nezamdost J. Prog. Theor. Phys., 2010, **124**: 1037
29 Van Der Woude A. International Review of Nuclear Physics: Electric and Magnetic Giant Resonances in Nuclei. River Edge: World Scientific, 1991
30 D E Teramond G F, Gabioud B. Phys. Rev. C, 1987, **36**: 691
31 Skopik D M et al. Phys. Rev. C, 1998, **24**: 1791
32 Schadow W, Nohadani O, Sandhas W. Phys. Rev. C, 2001, **63**: 044006